JOURNAL OF MATERIALS SCIENCE 33 (1998) 2111–2119

Cracking phenomena of brittle films in nanostructure composites analysed by a modified shear lag model with residual strain

M. YANAKA, Y. TSUKAHARA, N. NAKASO
Toppan Technical Research Institute, Sugito-machi, Kitakatsushika-gun, Saitama 345, Japan
N. TAKEDA
Center for Collaborative Research, The University of Tokyo, 4-6-1 Komaba, Meguro-ku, Tokyo 153, Japan

This paper proposes a modification to the shear lag model for multiple cracking of thin films in order to take into account the residual strain, and uses it to estimate the critical fracture strength of SiO_x films with thicknesses from 75 to 660 nm deposited on 12 μm-thick polyethylene terephthalate (PET) substrates. It was found that: (1) The difference of residual strains in the film and substrate increased as the thickness of the film decreased. (2) In both initial and multiple formation of cracks, SiO_x films failed at almost constant values of a critical stress ranging from 200 to 300 MPa when the thickness was larger than 200 nm, whereas below that it failed at higher values. © *1998 Chapman & Hall*

1. Introduction

Recent progress in thin film and polymer technology has made it possible to deposit very thin ceramic films ($10 \sim 100$ nm in thickness) on flexible polymer films. A total thickness of such composites currently developed ranges from 10 to 100 μm. These belong to a new class of composite materials which have characteristic lengths measured in nanometres and micrometres. One industrial application of such composite materials is a transparent gas barrier film [1] consisting of SiO_x films and a polyethylene terephthalate (PET) substrate which is, thanks to the deposition of the SiO_x films, capable of preventing oxygen and water vapour gases from penetrating through the films.

A shortcoming of such materials is that they are easily degraded when they are subjected to the stretching or bending force [1, 2] because the ceramic film is brittle and easy to break while the polymer substrate is soft and flexible. In order to correctly characterize the fracture strength, it is desired to establish a quantitative method of estimating the tensile fracture strength of such composite materials. Unfortunately, conventional methods, in which brittle films were detached from substrates and subjected to a tensile or bending test, cannot be used because the ceramic films are too thin.

As reported previously [3], multiple cracks perpendicular to the direction of the tensile force and in roughly uniform spacings are observed to emerge in the SiO_x film when the transparent gas barrier film is subjected to a tensile test (Fig. 1). This phenomenon is known to occur in composite materials consisting of brittle films adhering to high-elongation substrates, and a list of literature concerning with the phenomenon is found in a monograph by Wojciechowski *et al.* [4]. A shear lag model was adopted by Wojciechowski *et al.* [4] to explain the mechanism how the stress piled up in segmented films of Ni–Fe alloy adhering to a polyimide substrate. However, their model did not take into account the residual strain which might have affected the fracture process considerably. As described in the following sections, the residual strain really existed in our specimens, as in most cases of thin film deposition, and its effect could not be ignored. Using the shear lag model, Aveston *et al.* [5, 6] analysed extensively the multiple fractures in brittle fibres embedded in unidirectional fibre-reinforced composites and cross-ply laminates ($0^\circ/90^\circ/0^\circ$). They pointed out that the residual stress caused by the difference in thermal expansion coefficients of laminates with different fibre directions took an important role in the formation of initial small cracks.

Taking into account the residual stress, Hu *et al.* [7] developed a method based on the fracture mechanics to calculate the energy release rate associated with crack expansion in thin films. They obtained estimations for the model 1 fracture toughness (K_c^1) of chromium films deposited on aluminium and steel substrates. According to their analysis, a stress in the film at which the film failed was higher for specimens with thinner films if other experimental conditions were identical. On the contrary, it was assumed in the analyses by Wojciechowski *et al.* [4] and others [5, 6, 8] that the film should fail at a critical stress piled up

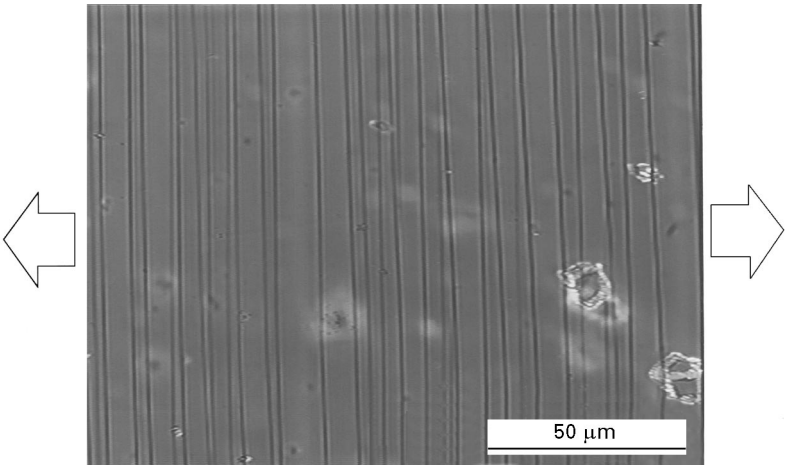

Figure 1 Observation of the multiple cracking of SiO_x thin film by optical microscopy. The direction of applied tensile force is shown by white arrows. The SiO_x film thickness and substrate strain were 215 nm and 6.3%, respectively.

in the film which was specific to the film material but regardless of the film thickness.

Therefore, it is quite interesting to study the following issues with such new class of specimens with brittle films tens of nanometer in thickness deposited on polymer substrates. (1) What is the quantity which characterizes the fracture strength of the brittle films in tensile tests? (2) Is it possible to describe the mechanism of both initial cracking and multiple cracking with a same model? (3) Is the residual strain correctly incorporated into the model? (4) Does the model quantitatively explain the experimental data? And to what extent? These questions are important in understanding the fracture process and in establishing a quantitative method of fracture strength measurements of not only nanocomposites but also micromachines and other applications of thin film technology to mechanical engineering.

This paper modifies the shear lag model used by Wojciechowski *et al.* [4] and takes into account the residual strains. The model is applied to analyse experiments on tensile tests of transparent gas barrier films consisting of SiO_x films deposited on PET substrates, and to quantitatively estimate the critical fracture stress in the SiO_x films whose thicknesses range from 75 to 660 nm.

2. Theory

2.1. Residual strains in the composite

Either because of the mismatch in the thermal expansion coefficients between the substrate and the film, or of the intrinsic volume change of the film during and after the evaporation process, the film-substrate composite under investigation in this paper resulted in a curl when it was cut into a ribbon-shape. (Fig. 2a)

Let us suppose that a composite plate consisting of a polymer substrate with a ceramic film is forced to be flat by the applied moment which cancels out the initial curl. We also assume that the strains in the substrate ε_s and in the film ε_f are uniformly distributed in the thickness direction. A one-dimensional model to be considered is shown in Fig. 2b. Thicknesses of

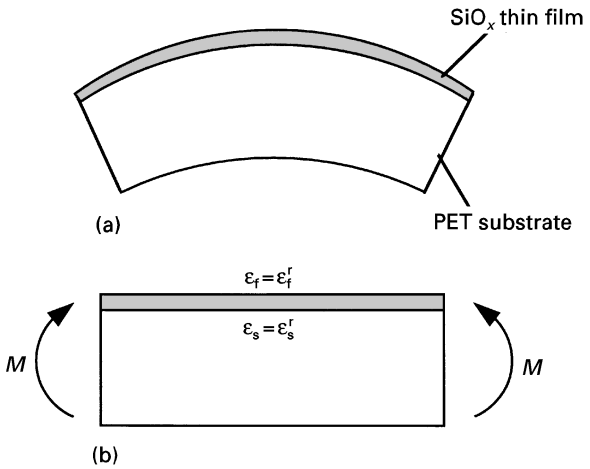

Figure 2 (a) Schematic showing the curl of a thin film/substrate strip due to residual strains. (b) The strip is forced to be flat by externally applied moment M.

the substrate and film are b and d, respectively. Stresses σ and strains ε in layers in this situation are residual components and be expressed with the superscript r as follows.

$$\sigma_f^r = E_f \varepsilon_f^r \tag{1}$$

$$\sigma_s^r = E_s \varepsilon_s^r \tag{2}$$

where E expresses Young's modulus and subscripts f and s stand for the thin film and the substrate, respectively.

A total force in the composite must be zero in this situation because it is not stretched yet. Thus,

$$E_f \varepsilon_f^r d + E_s \varepsilon_s^r b = 0 \tag{3}$$

2.2. Initial cracks

Next, let us suppose that the composite is subjected to a tensile test. As shown above, at the beginning of the tensile test, the film and substrate already have strains of ε_f^r and ε_s^r, respectively. But until initial cracks are induced in the film, the tensile load is transferred from the grips of the instrument to the film and substrate, and no interfacial shear stress between the film and

substrate exists. A load P_c applied to the composite is a sum of loads P_f and P_s transferred to the film and the substrate, respectively

$$P_c = P_f + P_s \tag{4}$$

Each load is related to a corresponding stress (residual plus applied)

$$P_c = \sigma_c(b + d)w \quad P_f = \sigma_f dw \quad P_s = \sigma_s bw \tag{5}$$

where w is a width of the composite plate. The subscript c stands for composite. Let us assume that the film and substrate are elastic, though not necessarily linearly elastic. Then

$$\sigma_f = E_f \varepsilon_f^{nc} = E_f(\varepsilon_c + \varepsilon_f^r) \tag{6}$$

$$\sigma_s = E_s \varepsilon_s^{nc} = E_s(\varepsilon_c + \varepsilon_s^r) \tag{7}$$

The superscript nc which means no crack exists in the film is shown to distinguish the present case from the analysis of multiple cracks described in the next section. It should be reminded that the Young's modulus E_s of the polymer substrate is a function of strain, and Equation 7 should be understood as a definition of the Young's modulus. With these expressions, Equation 4 is written in terms of the stress and strains

$$\sigma_c(b + d) = E_f(\varepsilon_c + \varepsilon_f^r)d + E_s(\varepsilon_c + \varepsilon_s^r)b \tag{8}$$

2.3. Multiple cracks (shear lag model)

In this section, let us consider the stress and strain when multiple cracks perpendicular to the load direction are induced in the film and the films are divided into many segments with equal widths L, as modelled in Fig. 3. Fig. 1 shows that this idealization is not very far from reality. Now the load applied by the instrument is not transferred directly to the film. However, the tensile stress in the film σ_f still exists as a consequence of a transfer across the interface of a shear stress τ_i into the film,

$$\sigma_f(x) = \frac{1}{d}\int_0^x \tau_i dx' \tag{9}$$

Here the elastic coupling is assumed at the interface. In turn, a part of the load which was supported by the film when there was no crack is now supported by the substrate. Thus, an additional stress $\overline{\Delta\sigma_s}$ is generated in the substrate,

$$\overline{\Delta\sigma_s}(x) = \overline{\sigma_s}(x) - E_s(\varepsilon_c + \varepsilon_s^r) \tag{10}$$

where $\overline{\sigma_s}(x)$ is a net tensile stress in the substrate, and the upper bars indicate that the quantities are averaged over the thickness of the substrate. At the place of the crack ($x = 0, L$) all the load is supported by the substrate, therefore $\overline{\Delta\sigma_s}$ takes its maximum value

$$\overline{\Delta\sigma_s}(x = 0, L) \equiv \overline{\Delta\sigma_0} = \frac{(b + d)}{b}\sigma_c - E_s(\varepsilon_c + \varepsilon_s^r) \tag{11}$$

An approximate formula for $\overline{\Delta\sigma_s}(x)$ was derived using a modified shear lag model described in detail in the

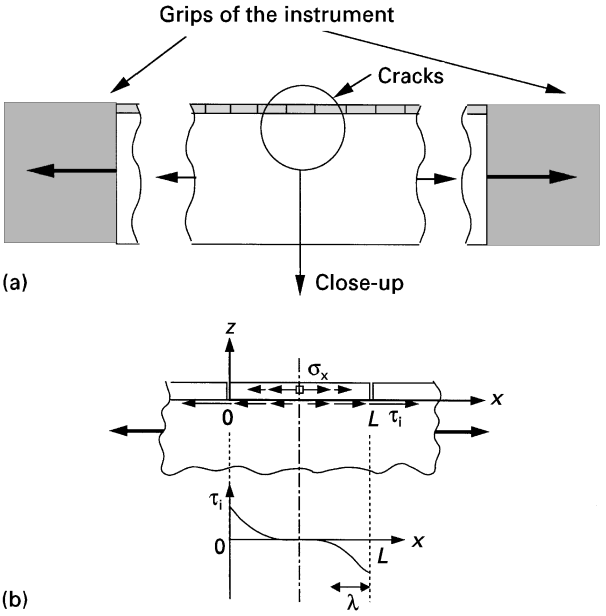

Figure 3 (a) A two-dimensional model for a layered substrate in the tensile test after multiple cracks are induced in the film. (b) A detail model of stress distributions around a cracked segment of the film. σ_f, τ_i and λ are tensile stress in the film, interfacial shear stress, and load transfer length, respectively.

Appendix

$$\overline{\Delta\sigma_s}(x) = \left(\overline{\Delta\sigma_0} + \frac{E_s E_f d\varepsilon''}{E_f d + E_s b}\right) \times (1 + e^{-L/\lambda})^{-1}(e^{-x/\lambda} + e^{(x-L)/\lambda}) - \frac{E_s E_f d\varepsilon''}{E_f d + E_s b} \tag{12}$$

where

$$\lambda = \left(\frac{2G_s(E_f d + E_s b)}{b^2 E_s E_f d}\right)^{-1/2} \tag{13}$$

$$\varepsilon'' = \varepsilon_c + \varepsilon_f^r - \frac{1}{E_f}\frac{b}{d}\overline{\Delta\sigma_0} \tag{14}$$

$G_s = E_s/(2(1 + \nu_s))$ is a shear modulus of the substrate.

From a simple force balance in the substrate, τ_i is related to $\overline{\Delta\sigma_s}$ by

$$\tau_i = -b\left(\frac{d\overline{\Delta\sigma_s}}{dx}\right) \tag{15}$$

Therefore, the interfacial shear stress τ_i is obtained by substituting Equation 12 into Equation 15

$$\tau_i(x) = \frac{b}{\lambda}\left(\overline{\Delta\sigma_0} + \frac{E_s E_f d\varepsilon''}{E_f d + E_s b}\right) \times (1 + e^{-L/\lambda})^{-1}(e^{-x/\lambda} - e^{(x-L)/\lambda}) \tag{16}$$

It is obvious from this equation that τ_i takes maximum and minimum values at edges of the segment, $x = 0$ and $x = L$, respectively. Its magnitude decreases rapidly toward inside of the segment within the distance λ (Equation 13) which is depicted as a load transfer length hereafter (See Fig. 3b). The tensile stress in the film is obtained by substituting Equation 16 into Equation 9. It takes a maximum value at

the centre of the segment

$$\sigma_f(L/2) = \frac{b}{d}\left(\overline{\Delta\sigma_0} + \frac{E_s E_f d\varepsilon''}{E_f d + E_s b}\right) \times (1 + e^{-L/\lambda})^{-1}(1 - e^{-L/(2\lambda)})^2 \quad (17)$$

When the applied load is increased and $\sigma_f(L/2)$ exceeds some critical value, a new crack is generated at the centre and the width of the segment becomes half, $L \to L/2$. That causes a stress relief in the segments. When the tension is increased again, cracks will occur midway between the present cracks. Although this process may be repeated further, the shear stresses at both ends of the segment begin to overlap as L becomes smaller than λ. This results in their partial cancellation, which in turn results in a decrease of the magnitude of σ_f and leads to a saturation in the crack density.

3. Experiments

3.1. Specimens

SiO_x thin films were deposited on PET substrates by vacuum evaporation with different thicknesses. Oxygen content x was about 1.7 measured by X-ray photoelectron spectroscopy. The thickness of the PET substrate was 12 ± 0.2 μm. Four kinds of specimens with SiO_x film thicknesses of 75, 123, 215, and 660 nm were prepared. Specimens with a rectangular shape, length and width of which were 100 mm and 9.46 mm, respectively, were cut out of each of four specimens and set to a tensile stage. A specimen of a PET substrate without SiO_x films was also prepared.

3.2. Experimental procedure

Fig. 4 shows a block diagram of the instrument for tensile tests. First, a specimen of PET substrate underwent a tensile test to record a stress–strain curve, and the Young's modulus of the substrate E_s and its strain dependence were obtained. Fig. 5 shows the stress and E_s as a function of the strain in room temperature. From a knee of the stress–strain curve, the yield strain of the PET substrate was determined to be about 2.2%. The stretching speed during the test was the same as those used in tests for SiO_x/PET specimens which are described below. It is noticed that a constant value of 0.44 was assumed as Poisson's ratio of the PET substrate in the following analysis [9].

Because of the residual strains in the film and the substrate, specimens cut out of SiO_x/PET specimens curled. The residual stress of thin film was compressive because the SiO_x films were always on the outside surface of the curl. The difference of the residual strains existing in the film and substrate were calculated from the radius of the curvature ρ

$$\varepsilon_s^r - \varepsilon_f^r = \frac{b^2}{6\rho d}\frac{E_s b + 4E_f d}{E_f(b + d)} \quad (18)$$

This expression basically followed the two-dimensional formula which had been derived for the thermal transformation of the CFRP cross-ply laminates [10]. $E_s = 4.7 \times 10^3$ MPa were used in the calculation. The

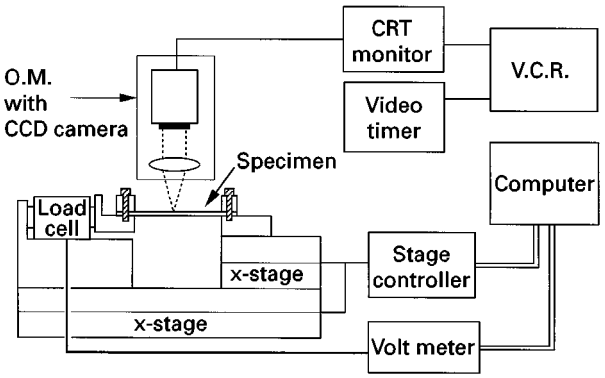

Figure 4 Block diagram of instruments used in the tensile test of specimens. To keep observing a same field during the test, the tensile stage as a whole was moved opposite direction to its displacement direction.

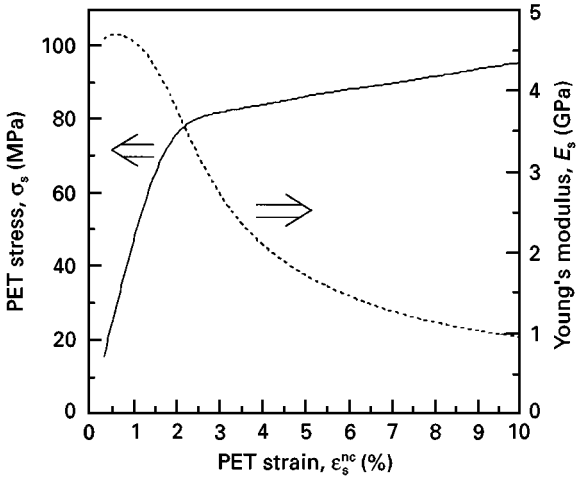

Figure 5 Experimental stress–strain curve (solid curve) and Young's modulus (dotted line) calculated from it by Equation 7 for a PET substrate without a film of SiO_x. Stretching speed of the specimen was 4.9 μm s^{-1}.

value of E_f will be estimated in the next section. From Equations 3 and 18 residual strains in the substrate and film can be calculated. Results are shown in Table I. The differences of the residual strains are larger in thinner films. The origin of this particular thickness dependence is not clarified yet, although it has often been reported [11, 12, 13] that the residual strains in evaporated SiO thin films were affected markedly by evaporation conditions such as the pressure, residual gases and temperature.

Next, tensile tests of the SiO_x/PET specimens were conducted, and observations with an optical microscope were made during the tests. Because the specimens curled, an initial composite stress σ_c of about 12 MPa was applied to stretch the specimens flat enough. After this initial stress was applied, the distance between two grips of the instrument that determined the effective length of the specimen was adjusted to be 46.85 mm for all specimens. Then, a mechanical stage to which one of the grips was attached was displaced at a constant speed of 4.9 μm s^{-1}. The relation between the stage displacement and the strain in the specimen was previously established by measuring the distance between two

TABLE I Estimated residual strains of the film and the substrate and their difference

SiO_x film thickness (nm)	$\varepsilon_s^r - \varepsilon_f^r$ (%)	ε_s^r (%)	ε_f^r (%)
660	0.24	0.08	− 0.16
215	0.48	0.07	− 0.41
123	0.63	0.05	− 0.58
75	1.01	0.06	− 0.96

TABLE II Estimated Young's moduli in SiO_x films deposited on PET substrates

SiO_x film thickness (nm)	Estimated Young's modulus (10^4 MPa)
660	4.0
215	4.8
123	3.7
75	4.8

thin lines printed on a specimen. In this manner, the strains in the specimens during the tests were obtained from the stage displacement. The applied load and the stage displacement were recorded in a computer every 5 s. Multiple fractures in the SiO_x films were observed by optical microscopy and recorded in a video cassette recorder (VCR) together with the count of a clock. The stress, strain and crack number were thus obtained during the test.

3.3. Experimental results

Let us summarize the test results. It should be reminded that ε_c had a non-zero value $\varepsilon_c = \varepsilon_c^i$ even at the beginning of a tensile test because the specimen had been stretched with an initial load. ε_c^i was estimated by solving Equation 8 in terms of ε_c. Parameters in Equation 8 necessary for the estimation were obtained as follows. Initial composite stress was $\sigma_c^i = (\text{initial load})/[(b + d)w]$ and substituted into σ_c. E_f was estimated by differentiating Equation 8 with respect to ε_c,

$$E_f = \frac{b+d}{d}\frac{d\sigma_c}{d\varepsilon_c} - \frac{b}{d}E_s \tag{19}$$

where $d\sigma_c/d\varepsilon_c$ was obtained as an average inclination of the stress–strain curve in a region with no cracks. Estimated values for E_f are found in Table II. Scatter in the values seems to represent the accuracy of the method instead of the film thickness dependence, so that an average value of 4.3×10^4 MPa was used in the following analysis regardless of the film thickness. It is worth pointing out that E_f estimated here is about 60% of the published values of about 7.2×10^4 MPa for bulk SiO_2 glasses [14].

Once a tensile test started, the specimen was further stretched and the apparent strain ε_c' estimated by measuring the relative elongation of the specimen during the test was obtained. A net strain of the composite was $\varepsilon_c = \varepsilon_c^i + \varepsilon_c'$ until initial cracks happened. The strain should have acquired x-coordinate dependence once the SiO_x film failed, because the specimen was no longer homogeneous in the x-direction. Then, $\varepsilon_c = \varepsilon_c^i + \varepsilon_c'$ must be understood as a virtual homogeneous strain which had been expected if there would have been no cracks.

Figure 6 shows the composite stress of the specimens as a function of the composite strain. All specimens showed yielding at about 2.0% of the composite strain, which roughly corresponds to the PET yield strain. A mean crack spacing $\bar{L}$ in the SiO_x film estimated from the number of cracks per unit length was shown as a function of the composite strain in Fig. 7. In the large strain region ($\varepsilon_c \sim 6\%$) in Fig. 7, one can see a tendency that the mean crack spacing was smaller for specimens with thinner SiO_x films; it was roughly proportional to the film thickness.

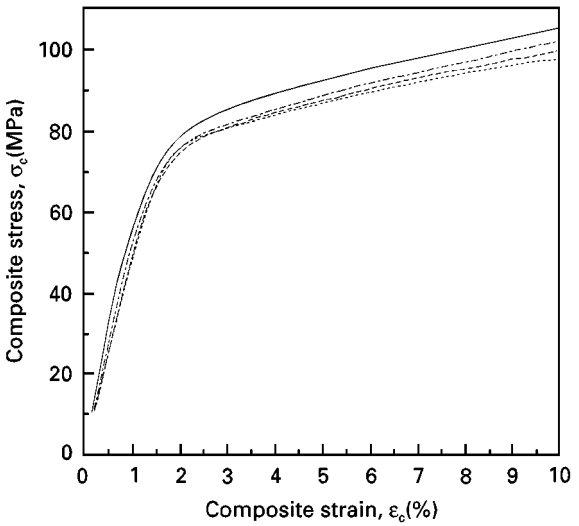

Figure 6 Experimental stress–strain curves for PET substrates with SiO_x films with different thicknesses. Stresses are composite stresses obtained by Equation 5. SiO_x film thicknesses: (····) 75 nm; (- - -) 123 nm; (–·–) 215 nm; (——) 660 nm.

Now let us consider the initial cracks. The crack onset composite strains were 0.69, 0.94, 1.20, and 1.84% for specimens with the SiO_x film thicknesses of 660, 215, 123, and 75 nm, respectively. The total stresses (residual plus applied) in the SiO_x films just before the crack onset were estimated using Equation 6. Results were shown in Fig. 8. It is noticed that the first cohesive failure in the SiO_x films occurred at almost same stresses when the thickness was larger than 200 nm, while below that the first failure occurred at higher stresses.

4. Shear lag analysis of multiple cracks in SiO_x films

In this section, a critical fracture strength of SiO_x films when a number of cracks were present is estimated according to the theory developed in Section 2.3. In the model it is idealized that cracks are evenly spaced in the film, parallel to each other and perpendicular to the direction of the tensile force, and new cracks emerge exactly at the centre of segments when the film

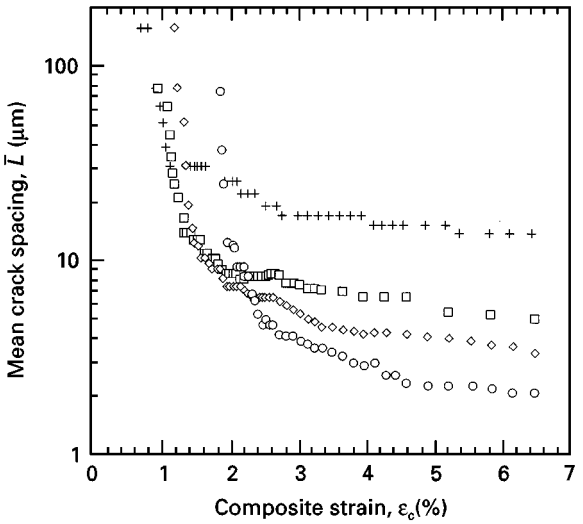

Figure 7 Experimental mean crack spacings in SiO_x films with different thicknesses deposited on PET substrates. The composite strains at which initial cracks were observed (mean crack spacings were largest) were different for different specimens because of the residual strains. SiO_x film thicknesses: (○) 75 nm; (◇) 123 nm; (□) 215 nm; (+) 660 nm.

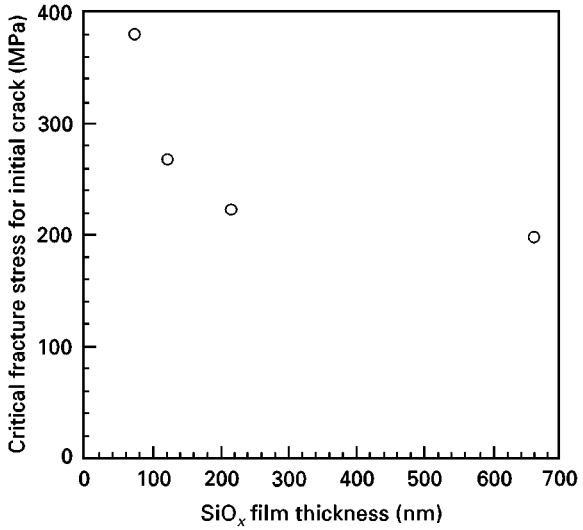

Figure 8 The critical stresses of SiO_x films at which initial cracks were observed, and its thickness dependence.

stress exceeds a critical value which is a definition of the critical fracture strength in the multiple cracks mode.

In the experiment, the number of cracks N which showed up in the field of the optical microscope was counted and a mean crack spacing $\bar{L}$ was deduced by the average $\bar{L} = O/N$ where O was the width of the field. In real specimens, the crack spacing had some statistical distribution around $\bar{L}$ as one can see in Fig. 1. The occurrence of the distribution might be attributed partly to defects irregularly distributed in the film and at the film/substrate interface which helped generate new cracks. At a given load, longest segments experience largest tensile stresses at their centres and therefore break into halves with more or less half lengths, while shorter segments remain unbroken (see Fig. 9). Hence, in a crude approximation the longest and shortest spacings L_{max} and L_{min}

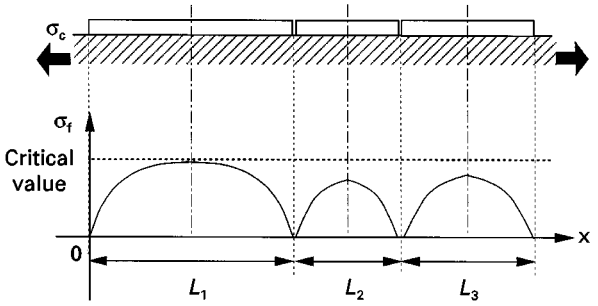

Figure 9 A conceptual illustration of the distribution of crack spacings. At a given load, the longest segment, L_1, experiences nearly critical stress at its centre, while shorter segments, L_2 and L_3, feel smaller values than the critical.

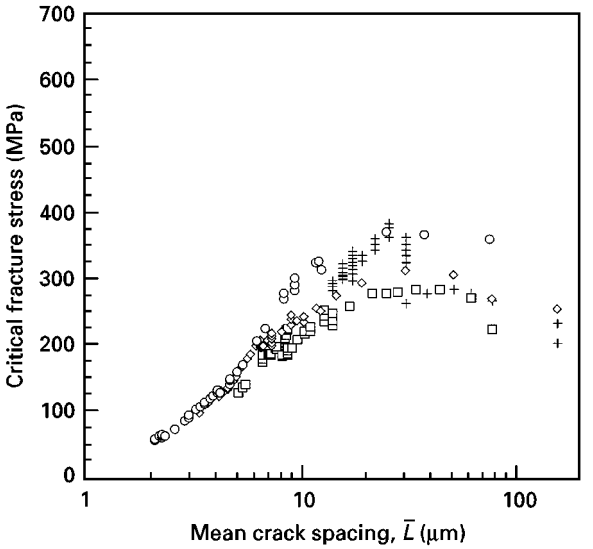

Figure 10 Estimations for critical fracture strength in SiO_x films deposited on PET substrates by means of a modified shear lag model. $\sigma_f(L/2)$ with $L = 4\bar{L}/3$ is plotted as a function of the mean crack spacing $\bar{L}$ because of a reason explained in Section 4. SiO_x film thicknesses: (○) 75 nm; (◇) 123 nm; (□) 215 nm; (+) 660 nm.

respectively will satisfy

$$\bar{L} \approx \frac{L_{max} + L_{min}}{2} \quad \text{and} \quad L_{max} \approx 2L_{min} \tag{20}$$

Therefore

$$L_{max} \approx \frac{4}{3}\bar{L} \tag{21}$$

The stress being experienced by the longest segments with $L = 4\bar{L}/3$ might be just below the critical fracture strength according to this approximation. For more accurate evaluation, the statistical distribution must be recorded and analysed in experiments.

In Fig. 10, $\sigma_f(L/2)$ with $L = 4\bar{L}/3$ is plotted as a function of the mean crack spacing $\bar{L}$. It is worth mentioning that most experimental data for different film thicknesses fit into a universal curve. From that curve it is also noticed that the estimations for the critical fracture strength fall in a range between 200 MPa and 400 MPa in a region of $L > 10$ μm. The specimen with the 75 nm-thick SiO_x film showed highest values in this region. These are consistent with the values estimated from initial cracks in Section 3.3.

Therefore, it seems to be plausible to assume that a same mechanism governed the generation of the initial cracks and multiple cracks in the SiO_x films.

5. Limitations of the model

Fig. 5 showed that PET substrates underwent plastic deformation at strains above 2.2%. This corresponds roughly to $\bar{L} \approx 8$ μm in Fig. 7 for specimens with SiO_x film thicknesses of 75, 123, and 215 nm. Therefore, the present model which assumes an elastic behaviour of all materials cannot be applied to $\bar{L} \leqslant 8$ μm. A marked decrease of the fracture strength estimations for these specimens in Fig. 10 for $\bar{L} \leqslant 8$ μm may be attributed to this limitation. However, the origin of a concave feature of the curve in Fig. 10 even for $\bar{L} > 8$ μm is still open for further investigation.

Researchers [5, 6, 7, 15] investigated the fracture mechanism of fibre-reinforced composites assuming that a shear stress at fibre/matrix interfaces took a constant value of the yielding shear stress. In our experiments, the crack spacing was found to be roughly proportional to the SiO_x film thickness at $\varepsilon_c \geqslant 6\%$ in Fig. 7. This behaviour is expected if there is a constant shear stress (a yielding shear stress) at the film/substrate interface. Thus, this line of reasoning will be useful to further investigate the fracture process of a brittle film on a polymer substrate after the substrate yields.

Furthermore, a local yielding of the substrate and a subsequent adhesive failure of the interface were conceivable at cracks and their neighbouring parts since the shear stress was concentrated around the cracks. A maximum interfacial shear stress τ_i at cracks ($x = 0$) was calculated by Equation 16 and compared with a yielding shear stress τ_y of the substrate, assuming well known formulas of Tresca ($\tau_y = (1/2)\sigma_y$) and von Mises ($\tau_y = (1/\sqrt{3})\sigma_y$) where σ_y is a uniaxial yielding stress of the substrate. σ_y was 78 MPa ($\varepsilon_s \sim 2.2\%$) for PET, and τ_y were 39 and 45 MPa by Tresca and von Mises formulas, respectively. Fig. 11 shows calculated $\tau_i(x = 0)$ for all specimens as a function of the mean crack spacing. The specimen with the 660 nm-thick SiO_x film showed an increase of $\tau_i(x = 0)$ at $\bar{L} < 30$ μm, and a maximum value was about 45 MPa. Therefore, a local yielding of the substrate near cracks was highly probable in the 660 nm-thick specimen at $\bar{L} \sim 30$ μm or less. Estimations of the fracture strength for the 660 nm-thick specimen at $\bar{L} < 30$ μm shown in Fig. 10 were therefore not correct. They were overestimated because the interfacial shear stress larger than the yielding shear stress was incorrectly assumed to transfer the tensile load to the film.

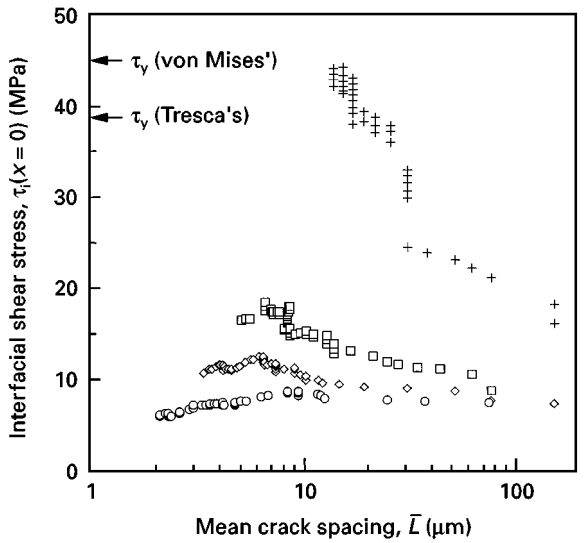

Figure 11 Estimations for the interfacial shear stress experienced by longest segments at their crack locations. The interfacial shear stress is expected to be maximum at cracks. SiO_x film thicknesses: (○) 75 nm; (◇) 123 nm; (□) 215 nm; (+) 660 nm.

During the tensile test, it was noticed that there was another type of fracture in the SiO_x film which were different from cracks investigated so far in this paper. [3]. That is the fractures which were caused by the compression of the film, the direction of which was perpendicular to the tensile force (Poisson's effect). To properly take this effect into account, a three-dimensional model will be needed for the analysis.

6. Conclusions

This paper proposed a crucial modification to the shear lag model for the multiple cracking of thin films in order to take into account the residual strain, and used it to estimate the critical fracture strength of SiO_x films with thicknesses from 75 to 660 nm deposited on 12 μm-thick PET substrates. It was found:

1. The difference of residual strains in the film and substrate increased as the thickness of the film decreased.
2. In both initial and multiple formation of cracks, SiO_x films failed at roughly constant values of a critical stress ranging from 200 to 300 MPa until about 200 nm, whereas below that it failed at higher values.
3. Some of discrepancies of the experimental data from the model can be qualitatively understood as caused by the yielding of the PET substrates.

It has long been discussed whether the tensile strength in thin films becomes larger or not when the film thickness is reduced, and some reported on the growing tendency of the tensile strength in deposited films of metals especially less than 100 nm in film thickness [16, 17, 18]. Present measurements for SiO_x films with thicknesses from 75 to 660 nm showed similar dependence on thickness. As briefly mentioned in the introduction, a fracture mechanical approach will be useful to consider the thickness dependence of the fracture strength. Its application is currently being investigated. It is remarkable that the estimated values of the critical fracture strength which lay in between 200 and 300 MPa were more than twice larger than published values for bulk SiO_2 glasses [14]. The proposed method will be especially useful for the measurement of films whose thickness is 1 μm or less because it would be very difficult to have a conventional tensile test of such thin films. It should be emphasized that the residual strains in layers have to be measured and used in the present model to achieve a reliable estimation.

A numerical approach will be needed when one wants to apply the present method to specimens with

multilayered structures or other complex geometry. Material properties of thin films, especially Young's modulus which critically affects the accuracy of fracture strength estimation, must be precisely measured which is another technical challenge being tackled currently.

Acknowledgements

The authors are grateful to Professor Takemoto of Aoyama-Gakuin University for many helpful discussions. Mr Okano, Director of the Technical Support Center of Toppan Technical Research Institute, and Mr Fujiu, Director of the Production Engineering Center of Toppan Technical Research Institute, are thanked for their support to the project.

References

1. J. RICE, *Food Process.* (1992) 78.
2. J. T. FELTS, in 36th Proceedings Annual Technical Conference of the Society of Vacuum Coaters (1993) p. 25.
3. M. YANAKA, N. NAKASO, Y. TSUKAHARA and N. N. HSU, *J. Acoust. Emiss.* **13** (1995) 23.
4. P. H. WOJCIECHOWSKI and M. S. MENDOLIA, "Physics of thin films" vol. 16, edited by M. H. Francombe and J. L. Vossen (Academic Press, San Diego, 1992).
5. J. AVESTON and A. KELLY, *J. Mater. Sci.* **8** (1973) 352.
6. *Idem., Phil. Trans. R. Soc. Lond.* A **294** (1980) 519.
7. M. S. HU and A. G. EVANS, *Acta Metall.* **37** (1989) 917.
8. K. W. GARRETT and J. E. BAILEY, *J. Mater. Sci.* **12** (1977) 157.
9. I. M. WARD, *J. Macromol. Sci.* B **1** (1967) 667.
10. N. TAKEDA and S. OGIHARA, *Compos. Sci. Technol.* **52** (1994) 183.
11. A. E. ENNOS, *Appl. Opt.* **5** (1966) 51.
12. M. A. NOVICE, *Br. J. Appl. Phys.* **13** (1962) 561.
13. A. E. HILL and G. R. HOFFMAN, *Br. J. Appl. Phys.* **18** (1967) 13.
14. W. D. KINGERY, H. K. BOWEN and D. R. UHLMANN, "Introduction to Ceramics" (John Wiley and Sons, New York, 1976).
15. A. KELLY and W. R. TYSON, *J. Mech. Phys. Solids* **13** (1965) 329.
16. H. LEIDHEISER, JR. and B. W. SLOOPE, *J. Appl. Phys.* **41** (1970) 402.
17. R. L. GRUNES, C. D'ANTONIO and F. K. KIES, *ibid.* **36** (1965) 2735.
18. A. CALTIN and W. P. WALKER, *ibid.* **31** (1960) 2135.

Received 9 December 1996
and accepted 17 December 1997

Appendix

A shear lag analysis [4] is modified to take into account the residual strains in layers. A model is two-dimensional as shown in Fig. 3. The x axis is taken in the plate direction and z axis in the depth direction. Let us assume a following relation for the additional substrate stress $\overline{\Delta\sigma_s}$ caused by the crack generation which was previously defined by Equation 10

$$\frac{d\overline{\Delta\sigma_s}}{dx} = H(\overline{\Delta\nu_s} - \Delta\nu_f) \tag{A1}$$

where $\overline{\Delta\nu_s}$ and $\Delta\nu_f$ are the additional displacements in the substrate and film respectively caused by the generation of cracks. They are

$$\overline{\Delta\nu_s} = \overline{\nu_s} - \nu_s^{nc} \tag{A2}$$

$$\Delta\nu_f = \nu_f - \nu_f^{nc} \tag{A3}$$

where ν_s^{nc} and ν_f^{nc} are the virtual displacements in the substrate and film respectively assumed if there were no cracks, and $\overline{\nu_s}$ and ν_f are the true displacements in the substrate and film, respectively, when cracks are generated. H is a factor that depends upon the geometry and the elastic properties of the materials. In the following, H is assumed to be a constant for simplicity.

Equation A1 signifies that the origin of the spatial rate of $\overline{\Delta\sigma_s}$, that is the interfacial shear stress (See Equation 15), is a difference between the displacement changes in the substrate and film caused by the generation of cracks. In the case of no residual strain, there is no difference between the displacements in the substrate and film when no cracks exist. That is $\nu_s^{nc} = \nu_f^{nc}$, and Equation A1 reduces to

$$\frac{d\overline{\Delta\sigma_s}}{dx} = H(\overline{\nu_s} - \nu_f) \tag{A4}$$

which is the same expression obtained by Wojciechowski [4].

Differentiating Equation A1 with respect to x

$$\frac{d^2\overline{\Delta\sigma_s}}{dx^2} = H\left(\frac{d\overline{\Delta\nu_s}}{dx} - \frac{d\Delta\nu_f}{dx}\right) \tag{A5}$$

To evaluate the right hand side of Equation A5, we introduce the following variables

$$\Delta\sigma_f(x) = \sigma_f(x) - E_f\varepsilon_f^{nc} \tag{A6}$$

$$\overline{\Delta\varepsilon_s}(x) = \overline{\varepsilon_s}(x) - \varepsilon_s^{nc} \tag{A7}$$

$$\Delta\varepsilon_f(x) = \varepsilon_f(x) - \varepsilon_f^{nc} \tag{A8}$$

where the meaning of subscripts, superscripts and bars are the same as before. In terms of these variables

$$\frac{d\overline{\Delta\nu_s}}{dx} = \overline{\Delta\varepsilon_s} = \frac{\overline{\Delta\sigma_s}}{E_s} \tag{A9}$$

$$\frac{d\Delta\nu_f}{dx} = \Delta\varepsilon_f = \frac{\Delta\sigma_f}{E_f} = \frac{1}{E_f d}\int_0^x \tau_i dx' - \varepsilon_f^{nc} \tag{A10}$$

The last expression is obtained by using the Equations A6 and 9. Substitution of Equation 15 into Equation A10 gives

$$\frac{d\Delta\nu_f}{dx} = \frac{b}{E_f d}[\overline{\Delta\sigma_s}(0) - \overline{\Delta\sigma_s}(x)] - \varepsilon_f^{nc} \tag{A11}$$

By making use of Equations A9 and A11, Equation A5 becomes

$$\frac{d^2\overline{\Delta\sigma_s}}{dx^2} - \phi\overline{\Delta\sigma_s} = H\varepsilon'' \tag{A12}$$

where

$$\phi = H\left(\frac{1}{E_s} + \frac{b}{E_f d}\right) \tag{A13}$$

$$\varepsilon'' = \varepsilon_f^{nc} - \frac{b}{E_f d}\overline{\Delta\sigma_s}(0) \tag{A14}$$

The solution to Equation A12 under the boundary condition of Equation 11 is

$$\overline{\Delta\sigma_s}(x) = \left(\overline{\Delta\sigma_0} + \frac{H\varepsilon''}{\phi}\right) \times (1 + e^{-L/\lambda})^{-1}(e^{-x/\lambda} + e^{(x-L)/\lambda}) - \frac{H\varepsilon''}{\phi} \tag{A15}$$

where $\lambda = 1/\sqrt{\phi}$.

Next, an expression for H will be sought. For simplicity, a constant shear stress τ_i is assumed through the thickness of the substrate. Hence

$$\frac{d\Delta w}{dz} = \frac{\tau_i}{G_s} \tag{A16}$$

where Δw is the additional displacement in the x-direction of the substrate. This assumption of a constant shear stress through the thickness in the substrate is apparently inconsistent, with a boundary condition that the shear stress must be zero at a free surface of the substrate. In fact, a bending force would be generated to cancel this shear stress at the free surface, which will be neglected hereafter for simplicity. $\Delta w = \Delta v_f(x)$ at the film/substrate interface, and $\Delta w = \overline{\Delta v_s}$ at $z = -b/2$. Hence, by integrating Equation A16 with respect to z

$$\overline{\Delta v_s} - \Delta v_f = -\frac{b\tau_i}{2G_s} \tag{A17}$$

Substituting Equation A17 into Equation A1 and then comparing it with Equation 15

$$H = \frac{2G_s}{b^2} \tag{A18}$$

Thus, Equation 12 is obtained by substituting Equation A18 into Equation A15.